Neurobiology of Aging 141 (2024) 102–112

Contents lists available at ScienceDirect

Neurobiology of Aging

journal homepage: www.elsevier.com/locate/neuaging.org

Hypothalamic MRI-derived microstructure is associated with neurocognitive aging in humans

Sandra Aleksic [a,*], Roman Fleysher [b,c], Erica F. Weiss [d], Noa Tal [e], Timothy Darby [f], Helena M. Blumen [d,g], Juan Vazquez [h], Kenny Q. Ye [i,j], Tina Gao [a], Shira M. Siegel [b], Nir Barzilai [a,k], Michael L. Lipton [b,l,1], Sofiya Milman [a,k,1]

[a] Department of Medicine, Institute for Aging Research, Albert Einstein College of Medicine, Bronx, NY, United States
[b] Department of Radiology, Columbia University Irving Medical Center, New York, NY, United States
[c] Department of Radiology, Albert Einstein College of Medicine, Gruss Magnetic Resonance Research Center, Bronx, NY, United States
[d] Department of Neurology, Albert Einstein College of Medicine, Bronx, NY, United States
[e] Department of Medicine, Cedars-Sinai, Los Angeles, CA, United States
[f] Albert Einstein College of Medicine, Bronx, NY, United States
[g] Department of Medicine, Albert Einstein College of Medicine, Bronx, NY, United States
[h] Department of Internal Medicine, John Hopkins University, Baltimore, MD, United States
[i] Department of Epidemiology and Population Health, Albert Einstein College of Medicine, Bronx, NY, United States
[j] Department of Systems and Computational Biology, Albert Einstein College of Medicine, Bronx, NY, United States
[k] Department of Genetics, Albert Einstein College of Medicine, Bronx, NY, United States
[l] Department of Biomedical Engineering, Columbia University, New York, NY, United States

ARTICLE INFO

Keywords:
Hypothalamus
Aging
Cortical thickness
Cognition
Human
Magnetic resonance imaging (MRI)

ABSTRACT

The hypothalamus regulates homeostasis across the lifespan and is emerging as a regulator of aging. In murine models, aging-related changes in the hypothalamus, including microinflammation and gliosis, promote accelerated neurocognitive decline. We investigated relationships between hypothalamic microstructure and features of neurocognitive aging, including cortical thickness and cognition, in a cohort of community-dwelling older adults (age range 65–97 years, n=124). Hypothalamic microstructure was evaluated with two magnetic resonance imaging diffusion metrics: mean diffusivity (MD) and fractional anisotropy (FA), using a novel image processing pipeline. Hypothalamic MD was cross-sectionally positively associated with age and it was negatively associated with cortical thickness. Hypothalamic FA, independent of cortical thickness, was cross-sectionally positively associated with neurocognitive scores. An exploratory analysis of longitudinal neurocognitive performance suggested that lower hypothalamic FA may predict cognitive decline. No associations between hypothalamic MD, age, and cortical thickness were identified in a younger control cohort (age range 18–63 years, n=99). To our knowledge, this is the first study to demonstrate that hypothalamic microstructure is associated with features of neurocognitive aging in humans.

1. Introduction

To ameliorate the rising global burden of aging-related morbidity, a better understanding of biological regulation of human aging is necessary. The hypothalamus, a collection of diencephalic nuclei responsible for neuroendocrine regulation of growth, reproduction, and maintenance of homeostasis, is emerging as a biological regulator of systemic aging (Leng et al., 2023; Sadagurski et al., 2017; Sadagurski et al., 2015a; Sadagurski et al., 2015b; Zhang et al., 2013b; Zhang et al., 2017). Several physiological functions altered in aging, including energy metabolism, circadian rhythms, stress response, and hormone release, are regulated by the hypothalamus. The hypothalamus also regulates several conserved neuroendocrine pathways implicated in longevity, including the growth hormone/insulin-like growth factor-1 (GH/IGF-1), thyrotropin, and gonadotropin pathways (Brown-Borg, 2007; Melmed, 2016). Given that the hypothalamic nuclei represent neuroanatomic

* Correspondence to: 1225 Morris Park Ave, Van Etten, ^{3}A–^{8}D, Bronx, NY, 10461, United States.
E-mail address: sandra.aleksic@einsteinmed.edu (S. Aleksic).
[1] Co-senior authors

https://doi.org/10.1016/j.neurobiolaging.2024.05.018
Received 8 August 2023; Received in revised form 17 May 2024; Accepted 31 May 2024
Available online 3 June 2024

substrates for the neuroendocrine pathways implicated in longevity, it is plausible that aging-related deterioration in the structure and function of the hypothalamus may promote systemic aging.

Several lines of evidence from animal models indicate that structural and functional changes that develop in the hypothalamus with aging may modulate systemic markers of aging and morbidity. Micro-inflammation and gliosis in the mediobasal hypothalamus, which develops with aging, was shown to play a causal role in accelerating whole body aging in mice, evidenced by reduced lifespan and health span, and accelerated neurocognitive decline (Leng et al., 2023; Zhang et al., 2013b). On the other hand, murine genetic models with extended lifespans, such as Ames dwarf, or those exposed to life-extending interventions, including caloric restriction, acarbose, 17-α estradiol and nordihydroguaiaretic acid, display reduced hypothalamic micro-inflammation and gliosis (Sadagurski et al., 2017; Sadagurski et al., 2015a; Sadagurski et al., 2015b). Additionally, aging-related reduction in SIRT-1 expression in the suprachiasmatic nucleus of the hypothalamus amplified aging-related circadian dysregulation (Chang and Guarente, 2013) and aging-related increase in mammalian target of rapamycin (mTOR) signaling in the hypothalamic proopiomelanocortin (POMC) neurons promoted weight gain in aged animals (Yang et al., 2012). This evidence from animal models supports the role of the hypothalamus in systemic aging and suggests that interventions aimed at restoring hypothalamic integrity may have potential to extend health span. Nonetheless, contributions of the hypothalamus to neurocognitive and systemic aging in humans remains unknown.

In humans, microstructural integrity in the hypothalamus can be non-invasively assessed with magnetic resonance imaging (MRI) (Thomas et al., 2019). Diffusion-weighted magnetic resonance (MR) imaging can track three-dimensional diffusion of water, which reflects microstructural central nervous system changes such as inflammation and gliosis (Alexander et al., 2007; Budde et al., 2011; Hagen et al., 2007). Mean diffusivity (MD), which reflects the direction-independent magnitude of diffusion, and fractional anisotropy (FA), which reflects directional cohesion of anisotropic diffusion, have been used to provide readings of the microstructure of subcortical gray matter regions (Abe et al., 2008), including the hypothalamus (Puig et al., 2015; Thomas et al., 2019). Higher MD in the hypothalamus, attributed to abnormal hypothalamic microstructure, has been associated with obesity (Thomas et al., 2019). However, studies that evaluated hypothalamic structure and function in aging humans are scarce. Several studies that assessed the association of hypothalamic diffusion with age provided contradictory results (Spindler and Thiel, 2022; Thomas et al., 2019). One cross-sectional study found no significant association between hypothalamic MR diffusion metrics and cognition. However, this study reported limited neurocognitive assessments and was not focused on individuals in the later decades of life, when neurocognitive aging accelerates (Spindler and Thiel, 2022). Thus, it remains unresolved whether deterioration in hypothalamic microstructure represents a feature of human aging and if hypothalamic microstructural integrity plays a role in neurocognitive aging.

Given the incomplete characterization of hypothalamic microstructure with chronologic and neurocognitive aging in humans, we investigated relationships among hypothalamic microstructure, age, and features of neurocognitive aging, including regional cortical thickness and cognition, in two cohorts of community-dwelling adults with ages spanning from adolescence into advanced old age.

2. Materials and methods

2.1. Study participants

2.1.1. LonGenity Brain MRI cohort

In the LonGenity Brain MRI cohort (n = 124), we investigated the relationships between hypothalamic MD and FA with age, cortical thickness, and cognition. The participants were enrolled into the LonGenity Brain MRI Study from an ongoing longitudinal cohort study, LonGenity (Gubbi et al., 2017). The LonGenity cohort is composed of Ashkenazi Jewish individuals aged 65 and older (n = 1225, 57 % female), half of whom are offspring of parents with exceptional longevity. Exclusion criteria for LonGenity are dementia at baseline and severe visual or hearing impairment, which would prevent participants from participating in study assessments. Participants undergo annual neurocognitive and clinical evaluations that include anthropometric measurements and collection of detailed medical histories. Education attainment is recorded at study baseline. Eligible participants, without a history of stroke, neurodegenerative disease, and traumatic brain injury, are recruited at their annual study visits into the LonGenity Brain MRI Study, focused on understanding the correlates of brain imaging and healthy aging. Blood samples are collected at the study visit when MRI is performed and hemoglobin A1c is measured.

2.1.2. Lifespan cohort

In the Lifespan cohort (n = 99), we investigated the relationships between hypothalamic MD and FA with age and cortical thickness. The Lifespan study was started at Albert Einstein College of Medicine with the aim to define structural and functional brain changes across the human lifespan and provide a database of normative imaging data for assessment of age-related changes of the brain. Study participants were recruited from the community and comprise healthy individuals (50 % female) aged 18–63 years. Exclusion criteria for Lifespan participants included history of head injury, psychiatric disease (bipolar disorder, schizophrenia, anxiety, depression), neurological disease, diabetes, heart disease, hypertension, and contraindication to MRI.

2.2. Neurocognitive assessments

The LonGenity cohort undergoes neurocognitive testing at annual study visits, including at the annual visit within three months of the brain MRI. Out of 124 LonGenity Brain MRI participants, at the time of this analysis 79 had at least one annual follow-up neurocognitive assessment performed at least one year after the MRI: In total, there were 249 annual neurocognitive assessments, including 124 at the time of the MRI and 125 after the MRI (Table S1), which were included in the exploratory analysis.

A structured neurocognitive battery of 8 tests was administered, which covered cognitive domains that included speed of processing, attention and executive functions (Trail Making Test Part A/Part B (Reitan, 1955), Digit Span (Wechsler, 1981), Digit Symbol (Wechsler, 1981)); verbal memory (Free and Cued Selective Reminding Test (Buschke et al., 1999; Buschke et al., 2006), Logical Memory (Wechsler, 1987)); and language (Phonemic and Category fluency (Goodglass and Kaplan, 1983), Boston Naming Test 15-item version (Stern et al., 1992)). Standardized (Z) scores were calculated for each of the 10 scores generated from the 8 tests. Appropriate standardized scores were averaged to create composite scores of overall and theoretical domain-specific (i.e., executive, memory, language, attention, and visuomotor) neurocognitive functioning (for test-domain mapping, see Supplementary Methods). An overall neurocognitive composite score which included standardized scores for each measure was used as a surrogate measure of overall neurocognitive functioning. For all neurocognitive composite scores, a higher value indicates better performance.

2.3. MRI acquisition

Brain MRI scanning in both study cohorts was performed with a Philips 3 T Ingenia Elition system using a 32-channel head coil (Philips Medical Systems, Best, Netherlands) at the Albert Einstein College of Medicine. A board-certified neuroradiologist (MLL) reviewed all images for incidental findings and visible signs of prior significant neurological disease (e.g., stroke, encephalitis, hemorrhage) were recorded.

Participants with incidental pathologic findings in the region of the hypothalamus were excluded. Detailed description of MRI acquisition protocol is available in Supplementary Data.

2.4. Image processing

2.4.1. Image processing pipeline infrastructure

A custom framework (RoboDuct) was used to efficiently generate analysis-specific data processing pipelines leveraging optimal FSL (Jenkinson et al., 2012; Smith et al., 2004; Woolrich et al., 2009), AFNI (Cox, 1996), ANTs (Avants et al., 2011; Avants et al., 2014; Tustison et al., 2014), FreeSurfer (Dale et al., 1999; Desikan et al., 2006) and other libraries. Basic operations (e.g., EPI distortion correction, registration using white matter (Greve and Fischl, 2009), brain extraction) have been implemented as in the Human Connectome Project (Glasser et al., 2013). RoboDuct inserts check points for manual validation where its modules might perform suboptimally (e.g., brain extraction). Diffusion-weighted imaging (DWI) data underwent motion and eddy current correction and EPI distortion correction followed by diffusion tensor imaging (DTI) fit to generate standard DTI parameters. The DTI parameter maps were registered to T1 weighted image using rigid body transformations for subsequent region of interest (ROI) analyses (Fleysher et al., 2018).

2.4.2. Hypothalamic delineation

A most-probable atlas of the hypothalamus was generated using the following procedure: First, we selected brain MRI images of 18 older adults from the LonGenity Brain MRI study (50 % female). Under the supervision of a neuroradiologist (MLL), three raters (SA, NT, TD) performed manual delineation of the hypothalamus on T1-weighted coronal images using the ITK-SNAP polygon tool, according to established anatomical landmarks (Chen et al., 2021). All raters were trained on relevant anatomy, landmarks to be used for the delineations, and ITK-SNAP software tools prior to beginning of any work related to generating the most-probable hypothalamus atlas. Each rater delineated 12 MRI scans, thus each of the 18 scans was delineated by two raters. Dice index was calculated to assess the degree of spatial overlap between hypothalamic regions delineated by two raters (Dice index = 2*volume of overlap / (sum of volumes of two regions); values range: 0–1, with higher value meaning higher agreement). Median Dice index for agreement between the raters was 0.85 (range 0.72–0.93). Next, the 36 manually delineated masks of 18 hypothalami were transformed to the template image of the youngest participant in the LonGenity Brain MRI dataset (65-year-old male), using nonlinear registration. Each pixel on the template was assigned one of three labels (left hypothalamus, right hypothalamus, outside of the hypothalamus) based on majority vote of the raters' 36 masks. The pixels that were assigned a label within the hypothalamus based on the majority vote were included in the most-probable hypothalamus atlas. Hypothalamus was delineated in each individual by transforming the most-probable hypothalamus atlas to the individual's T1-weighted volume. These masks were compared to the manually delineated masks in 10 (5 female) randomly selected LonGenity Brain MRI study participants using Dice index, which showed good agreement (median 0.76, range 0.60–0.85; Figure 1). Other anatomical ROIs (amygdala, hippocampus, cerebral cortical regions) on individual T1 weighted images were delineated using ASEG and WMPARC modules of FreeSurfer version 6.0 (Dale et al., 1999; Desikan et al., 2006). Average of DTI metrics (MD FA) were computed for all voxels within the hypothalamus, amygdala, and hippocampus on each side. For each ROI, volume-weighted means of average MD and FA for right and left were generated and used in further analyses.

Given the proximity of the hypothalamus to the cerebrospinal fluid (CSF), we tested whether hypothalamic-CSF partial volume effects in the edge voxels (Figure S1) could explain observed associations between hypothalamic DTI metrics and age. We performed a sensitivity analysis in which an "eroded" hypothalamic mask was created, which excluded 2 voxels at the interface of the hypothalamic margin and the CSF. To generate the eroded hypothalamic mask, synthStrip module of FreeSurfer was first used to remove non-brain tissue. From the remaining brain mask, the 3rd ventricle, delineated by FreeSurfer, was removed. The remaining brain mask was eroded by 2 mm and intersected with our hypothalamic mask to obtain the portion of the hypothalamus which is at least 2 mm from the hypothalamic-CSF margin.

2.4.3. Cortical thickness

Regional cortical thickness was measured using FreeSurfer version 6.0 in LonGenity Brain MRI Cohort (Dale et al., 1999; Desikan et al., 2006) and FreeSurfer 7.1 in Lifespan. The entire cerebral cortex was segmented into 34 cortical regions in each hemisphere, based upon the Desikan-Killiany atlas (Desikan et al., 2006). Mean cortical thickness in each of the 34 cortical regions of the left and right hemisphere were added (i.e. collapsed), to reduce the number of statistical models to be performed given that no hemisphere-specific analyses were planned. Collapsed cortical regions were grouped into cerebral lobes (Klein and Tourville, 2012) (Supplementary Data). Overall white matter lesions burden was estimated based on white matter hypointensities measure which is automatically computed from T1-weighted images by FreeSurfer. Additionally, in 115 of 124 LonGenity participants, semi-quantitative ratings of white matter hyperintensities generated from T2W-FLAIR images with Age-Related White Matter Changes scale (ARWMC) (Wahlund et al., 2001) were used to calculate a global white matter hyperintensity burden score as an alternative measure of white matter lesion burden (Supplementary Methods).

2.5. Statistical analysis

2.5.1. Cross-sectional analysis

Normality was assessed by inspection of the histograms and by Shapiro-Wilk test with a two-tailed p-value threshold of < 0.05. MD and FA metric values were transformed into z-scores (zMD and zFA, respectively). The associations between age (predictor) and hypothalamic zMD and zFA (outcomes) were assessed using univariable and sex-

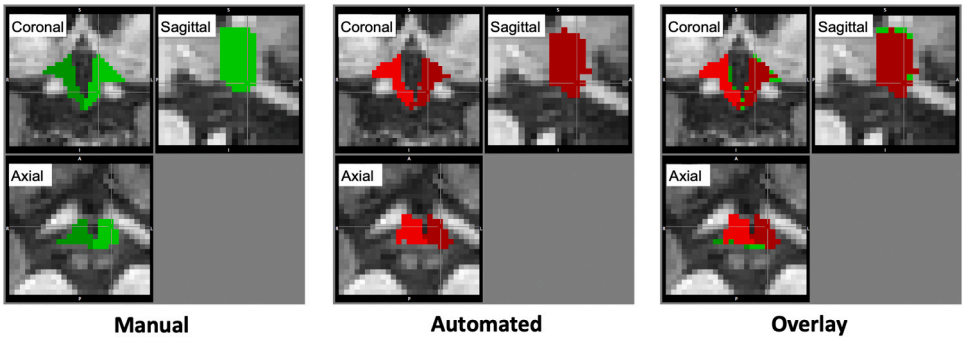

Fig. 1. Comparison of the manual and automated delineation of the hypothalamus in a representative LonGenity Brain MRI cohort participant.

adjusted multivariable linear regression models. The associations between hypothalamic zMD and zFA (predictors) with regional cortical thickness measures and overall and domain-specific neurocognitive scores (outcomes) were assessed using multivariable linear regression, with age, sex, education years, estimated total intracranial volume (eTIV) and the overall white matter lesion burden as covariates. For the associations with cortical thickness in 34 brain regions, we first performed multivariate multivariable general linear models (GLMs), with either MD or FA as predictors of interest, followed by univariate multivariable GLMs; univariate GLMs were only interpreted if the overall multivariate GLM models were significant ($p < 0.05$). We included adjustments for overall white matter lesion burden measure in order to determine if the observed associations between hypothalamic DTI metrics, regional cortical thickness, and cognition were above and beyond previously observed relationships between cerebral cortical atrophy and white matter lesions with aging (Habes et al., 2016; Wen et al., 2006). Given prior reports of the associations between hypothalamic DTI metrics and obesity (Thomas et al., 2019), impaired glucose metabolism (Rosenbaum et al., 2022), and hypertension (Purkayastha et al., 2011a), we tested the associations of hypothalamic zMD and zFA with body mass index (BMI), hemoglobin A1c, and history of diabetes and hypertension, in age and sex-adjusted linear regression models; given that we did not find significant associations ($p > 0.05$, Table S2), these variables were not included as covariates in the models. Assumptions for linear regression were assessed and met, including normality, homoscedasticity, linearity, and absence of multicollinearity, influential observations, and specification errors.

2.5.2. Sensitivity analysis

To determine if the observed cross-sectional associations between hypothalamic DTI metrics and regional cortical thickness and neurocognitive scores could be confounded by a generalized deterioration of the microstructure of the limbic system, to which the hypothalamus belongs, we performed sensitivity analyses which included additional adjustment for zMD and zFA of the hippocampus and amygdala, which are subcortical gray matter structures in the limbic system that are involved in cognition and demonstrate microstructural alterations with aging (den Heijer et al., 2012; Jiang et al., 2019).

To assess whether observed age-associations of hypothalamic diffusion metrics could result from age-biased CSF-partial volume effects (above), we ran univariable linear regression models to evaluate for dependence of hypothalamic volume on age and hypothalamic diffusion parameters. Additionally, we repeated analysis of associations between age (predictor) and hypothalamic zMD and zFA (outcomes) but limited to the region of the hypothalamus distant from the CSF (eroded hypothalamus above).

2.5.3. Longitudinal analysis

All available annual neurocognitive assessments, which included 124 assessments at the time of the MRI and 125 assessments performed at least one year after the MRI, were analyzed using linear mixed effect models, with individual intercept as the random effect and the common age effect for all subjects. The main fixed effect predictor was hypothalamic zMD/hypothalamic zFA. Additional covariates included in the models were sex, education, white matter hypointensities, eTIV, and whole-brain cortical thickness. The computation was performed using R library lme4, and the statistical significance were assessed using the likelihood ratio tests.

Statistical analysis was performed using STATA software, version 15 (StataCorp LP, College Station, TX) and R language (R version 4.3.2; R Foundation for Statistical Computing). A two-tailed Benjamini-Hochberg (BH) - adjusted p-value < 0.05 (Yekutieli and Benjamini, 1999), was considered statistically significant.

The LonGenity study was approved by the institutional review board (IRB) at the Albert Einstein College of Medicine. The Lifespan study was approved by the IRB at the Albert Einstein College of Medicine and Columbia University. Informed consent was obtained from all study participants.

3. Results

3.1. Hypothalamic microstructure varies with age and sex in older, but not younger adults

Characteristics of the LonGenity Brain MRI and Lifespan cohorts are presented in Table 1 and Table S3, respectively. In sex-adjusted analysis, age was significantly positively associated with hypothalamic zMD in the LonGenity Brain MRI cohort (beta [95 % CI] = 0.04 [0.01, 0.06], p = 0.005), but not in the Lifespan cohort (Table S4 and Figure 2a, c). There were no significant associations between age and hypothalamic zFA in either cohort (Table S4, Figure 2b, d). In age-adjusted models, sex was not significantly associated with hypothalamic zMD in either cohort, while men had lower hypothalamic zFA compared to women in the LonGenity Brain MRI cohort (beta [95 % CI] for male sex = −0.42 [−0.78, −0.07], p = 0.02), but not the Lifespan cohort (Table S4).

In sensitivity analysis, we found no statistically significant association between hypothalamic volume and age or hypothalamic volume and hypothalamic diffusion parameters (Table S5). MD of the eroded hypothalamic mask, despite representing only 28 % of the average hypothalamic volume located away from the CSF, demonstrated positive trend with age similar to the one observed with the MD of the entire hypothalamus (Pearson's correlation coefficient r = 0.15, p = 0.10; Figure S2).

3.2. Hypothalamic microstructure is associated with regional cortical thickness in older, but not younger adults

In models adjusted for age, sex, years of education, estimated total intracranial volume, and white matter hypointensities, zMD in the hypothalamus was negatively associated with average frontal lobe, parietal lobe, and cingulate cortical thickness in LonGenity Brain MRI cohort (beta [95 % CI], BH-adjusted p values): –0.06 [−0.10, −0.02], 0.008;

Table 1
LonGenity Brain MRI Study Participant characteristics (n=124).

Demographics	
Age (years)	78.7 (74.3, 83.4)
Sex, female (%)	58
Familial longevity (%)	59
BMI (kg/m^2), n=108	26.4 (23.9, 29.2)
HbA1c (%), n=105	5.5 (5.4, 5.8)
Education (years)	18 (16, 20)
Diabetes mellitus %, n=123	11
Hypertension %, n=122	48
Cancer %	38
Cardiovascular disease %, n=107	16
Neurocognition composite scores	
Overall, n=120	0.19 (-0.05, 0.64)
Executive, n=122	0.23 (-0.20, 0.72)
Memory, n=123	0.39 (-0.14, 0.67)
Language, n=121	0.24 (-0.16, 0.75)
Attention, n=123	0.21 (-0.23, 0.64)
Visuomotor, n=123	0.23 (-0.24, 0.75)
MRI metrics of lobar cortical thickness (mm)	
Frontal	4.7 ± 0.21
Parietal	4.3 ± 0.22
Temporal	5.2 ± 0.25
Occipital	3.6 ± 0.19
Cingulate	5.2 ± 0.28
MRI diffusion metrics in the hypothalamus	
Mean diffusivity (MD; mm^2/s)	0.00127 ± 0.000144
Fractional anisotropy (FA)	0.27 ± 0.034

Continuous data are represented as median (interquartile range) or means ± standard deviation. Where denoted, number indicates number of participants with available data where data are missing.

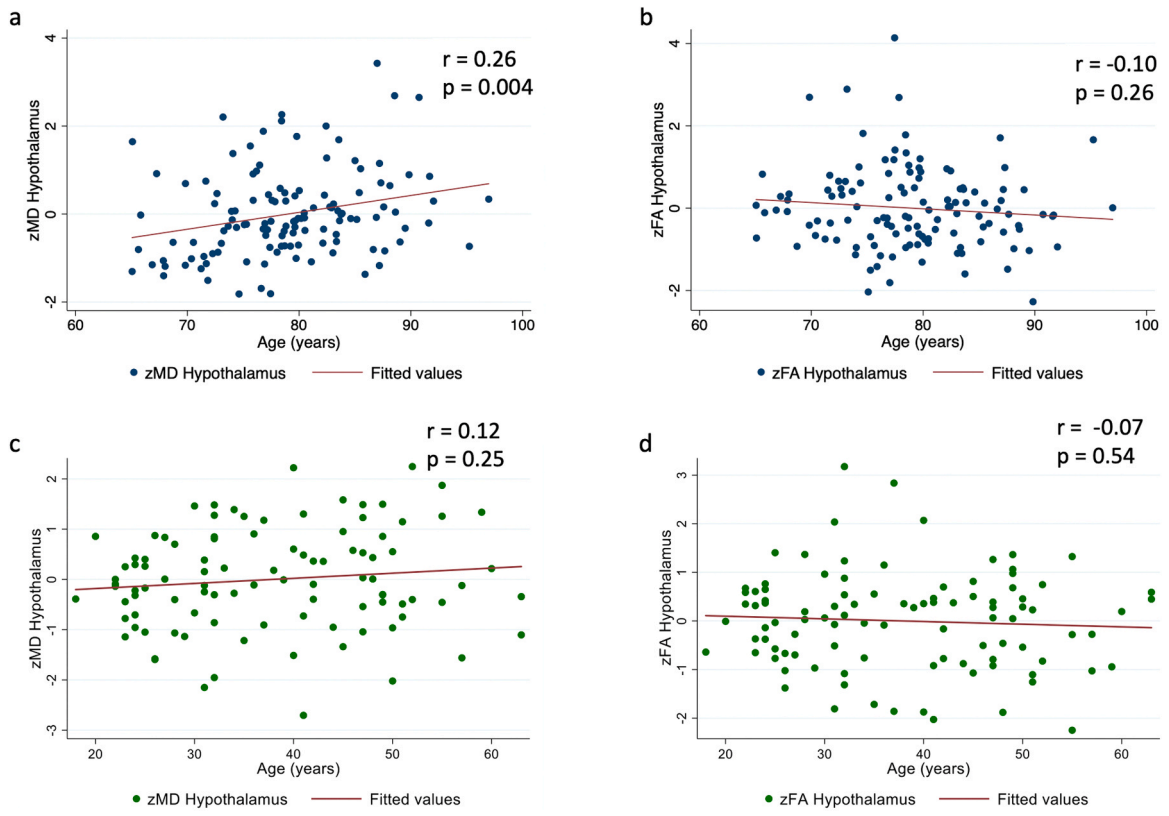

Fig. 2. Associations between age and z-scores of hypothalamic mean diffusivity (zMD; panel a, c) and fractional anisotropy (zFA; panel b, d) in LonGenity Brain MRI (a, b, n = 124) and Lifespan (c, d, n = 99) cohorts; r- Pearson's correlation coefficient.

−0.07 [−0.10, −0.03], 0.005; −0.07 [−0.12, −0.02], 0.01, respectively; Table 2). The represented multivariable linear regression models explained between 8 % and 22 % of the variability of the lobar cortical thickness (R^2), with hypothalamic zMD explaining 6–7 % of the variability (delta R2). The results were similar when white matter hyperintensities burden score was used to estimate white matter lesion burden instead of white matter hypointensities (Table S6). The analysis of the 34 anatomical subregions demonstrated that zMD in the hypothalamus was negatively associated with cortical thickness across regions within all cerebral lobes, with 12 out of 34 examined regions surviving correction for multiple testing (Table 3). The greatest effect size was observed in the medial orbitofrontal, frontal pole and rostral anterior cingulate regions (beta [95 % CI], BH-adjusted p values: –0.13 [–0.19, –0.06], 0.03; –0.12 [–0.20, –0.04], 0.03; –0.12 [–0.20, –0.04], 0.02, respectively; Table 3). Including zMD from the two other limbic regions, hippocampus and amygdala, in these models did not substantially alter the observed negative associations between zMD in the hypothalamus and regional cortical thickness (Tables S7, S8). In Lifespan cohort, no significant associations were found between hypothalamic zMD and lobar cortical thickness (Table S9). Hypothalamic zFA was not significantly associated with cortical thickness in either LonGenity Brain MRI (Table S10) or Lifespan cohort (data not shown).

Table 2
Associations between mean diffusivity (MD) in the hypothalamus and lobar cortical thickness in the LonGenity Brain MRI cohort.

Lobar cortical region	Beta (95 % CI)	p	BH-p	R^2	Delta R^2
Frontal	**-0.06 (-0.10, -0.02)**	**0.005**	**0.008**	**0.08**	**0.06**
Parietal	**-0.07 (-0.10, -0.03)**	**0.001**	**0.005**	**0.22**	**0.07**
Temporal	-0.04 (-0.08, 0.01)	0.13	0.128	0.11	0.02
Occipital	-0.03 (-0.06, 0.00)	0.07	0.084	0.18	0.02
Cingulate	**-0.07 (-0.12, -0.02)**	**0.004**	**0.01**	**0.21**	**0.06**

Multivariable linear regression, adjusted for age, sex, years of education, estimated total intracranial volume and white matter hypointensities (n = 124). Beta estimates are represented per 1 standard deviation of MD in the hypothalamus, BH-p: Benjamini-Hochberg - adjusted p-value, R^2 - standard R^2 of the model, Delta R^2 - increase in model R^2 due to addition of hypothalamic MD. BH-adjusted p-values were calculated using the set of raw p-values represented in the Table.

3.3. *Hypothalamic microstructure is associated with cognition independent of cortical thickness in older adults*

3.3.1. *Cross-sectional analysis*

Hypothalamic zFA was positively associated with the overall neurocognitive composite score (Figure 3b), which persisted after adjustments for age, sex, years of education, estimated total intracranial volume, and white matter hypointensities (beta [95 % CI] = 0.16 [0.07, 0.25], BH-adjusted p value = 0.006; Table 4). The represented regression model explained 32 % of the variability in the overall neurocognitive composite score (R^2), with hypothalamic zFA explaining 7 % of the variability (delta R^2); the effect size on the overall cognition per 1 SD of FA was equivalent to ~8 years younger age. Analysis by individual neurocognitive domains, found that zFA in the hypothalamus had significant positive associations with all domain-specific scores except visuomotor speed (BH-adjusted p value = 0.053), with greatest relative effect size on the executive and language domain scores (beta [95 % CI], BH-adjusted p value: 0.16 [0.02, 0.30], 0.029; 0.17 [0.03, 0.30], 0.03, respectively; Table 4). Given the observed associations between hypothalamic microstructure and cortical thickness, we added whole-brain cortical thickness to the model, which did not alter the observed positive association between zFA and neurocognitive composite scores (Table 4). Additionally, replacing white matter hypointensities with

Table 3
Associations between mean diffusivity (MD) in the hypothalamus and regional cortical thickness in the LonGenity Brain MRI cohort.

Regional cortical thickness	Beta (95 % CI)	p	BH-p	R^2	Delta R^2	Regional cortical thickness	Beta (95 % CI)	p	BH-p	R^2	Delta R^2
Frontal lobe						***Temporal lobe***					
Superior frontal	-0.05 (-0.10, 0.00)	0.06	0.10	0.11	0.03	Parahippo-campal	0.03 (-0.07, 0.14)	0.554	0.63	0.08	0.00
Caudal middle frontal	-0.02 (-0.06, 0.03)	0.497	0.58	0.07	0.00	Entorhinal	-0.04 (-0.17, 0.10)	0.607	0.64	0.08	0.00
Rostral middle frontal	-0.04 (-0.08, 0.00)	0.063	0.10	0.06	0.03	Temporal pole	-0.03 (-0.13, 0.08)	0.587	0.64	0.08	0.00
Pars opercularis	-0.02 (-0.07, 0.02)	0.273	0.36	0.09	0.01	Superior temporal	-0.05 (-0.10, 0.00)	0.054	0.10	0.18	0.03
Pars triangularis	**-0.06 (-0.11, -0.02)**	**0.006**	**0.023**	**0.11**	**0.06**	Middle temporal	-0.05 (-0.10, 0.00)	0.043	0.09	0.09	0.03
Pars orbitalis	-0.05 (-0.12, 0.01)	0.107	0.16	0.07	0.02	Inferior temporal	**-0.07 (-0.12, -0.03)**	**0.001**	**0.011**	**0.14**	**0.08**
Lateral orbitofrontal	-0.06 (-0.12, −0.01)	0.028	0.06	0.09	0.04	Transverse temporal	0.00 (-0.06, 0.07)	0.962	0.96	0.18	0.00
Medial orbitofrontal	**-0.13 (-0.19, -0.06)**	**0.0009**	**0.031**	**0.15**	**0.10**	Banks sup. temp. sulcus	-0.04 (-0.10, 0.01	0.093	0.14	0.15	0.02
Precentral	-0.03 (-0.08, 0.02)	0.17	0.23	0.15	0.01	Fusiform	**-0.08 (-0.13, -0.03)**	**0.002**	**0.014**	**0.21**	**0.07**
Paracentral	-0.04 (-0.09, 0.01)	0.134	0.19	0.09	0.02	***Occipital lobe***					
Frontal pole	**-0.12 (-0.20, -0.04)**	**0.006**	**0.026**	**0.12**	**0.06**	Lateral occipital	**-0.06 (-0.11, -0.01)**	**0.012**	**0.037**	**0.23**	**0.04**
Parietal lobe						Pericalcarine	-0.01 (-0.05, 0.03)	0.65	0.67	0.05	0.00
Postcentral	-0.05 (-0.09, −0.01)	0.022	0.06	0.12	0.04	Lingual	-0.04 (-0.07, 0.00)	0.048	0.09	0.23	0.03
Superior parietal	-0.06 (-0.11, −0.01)	0.022	0.05	0.17	0.04	Cuneus	-0.02 (-0.06, 0.02)	0.374	0.45	0.09	0.01
Inferior parietal	**-0.07 (-0.12, -0.03)**	**0.001**	**0.017**	**0.25**	**0.08**	***Cingulate***					
Supra-marginal	**-0.07 (-0.12, -0.03)**	**0.002**	**0.011**	**0.18**	**0.07**	Caudal ant. cingulate	-0.05 (-0.14, 0.04)	0.289	0.36	0.16	0.01
Precuneus	**-0.08 (-0.12, -0.03)**	**0.001**	**0.009**	**0.26**	**0.08**	Rostral ant. cingulate	**-0.12 (-0.20, -0.04)**	**0.004**	**0.019**	**0.15**	**0.06**
Insula	**-0.08 (-0.15, -0.02)**	**0.013**	**0.037**	**0.08**	**0.05**	Posterior cingulate	-0.05 (-0.10, −0.01)	0.025	0.06	0.12	0.04
						Isthmus cingulate	**-0.07 (-0.13, -0.02)**	**0.012**	**0.041**	**0.24**	**0.04**

Multivariable linear regression, adjusted for age, sex, years of education, estimated total intracranial volume and white matter hypointensities (n = 124). Beta estimates are represented per 1 standard deviation of MD in the hypothalamus, BH-p: Benjamini-Hochberg - adjusted p-value, R^2 - standard R^2 of the model, Delta R^2 - increase in model R^2 due to addition of hypothalamic MD. BH-adjusted p-values were calculated using the set of raw p-values represented in the Table.

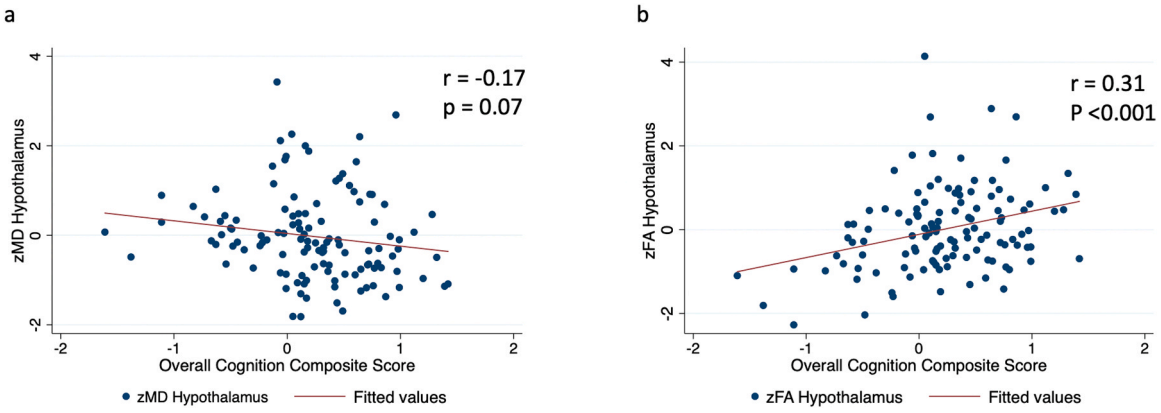

Fig. 3. Associations between overall cognitive composite scores (a higher score indicates better performance) and hypothalamic z-scores of mean diffusivity (zMD; panel a) and fractional anisotropy (zFA; panel b), (n = 120); r - Pearson's correlation coefficient (Pearson's correlation).

semi-quantitative white matter hyperintensities burden score, did not meaningfully change the results (Table S11). Including zFA from the two other studied limbic regions, hippocampus and amygdala, in the models did not meaningfully alter the results (Table S12). In unadjusted model, there was no statistically significant association between zMD in the hypothalamus and overall neurocognitive composite (Figure 3a). In multivariable models, hypothalamic zMD was negatively associated with language domain cognitive scores (beta [95 % CI] = −0.16 [−0.31, −0.02], p = 0.028), but this association did not survive adjustment for multiple testing (Table S13).

3.3.2. *Longitudinal analysis*

Out of 124 LonGenity Brain MRI participants, 79 had at least one annual follow-up neurocognitive assessment performed at least one year

Table 4
Associations between fractional anisotropy (FA) in the hypothalamus and neurocognition scores.

	Model A					Model B				
Composite score	Beta (95 % CI)	p	BH-p	R^2	Delta R^2	Beta (95 % CI)	p	BH-p	R^2	Delta R^2
Overall Cognition	**0.16 (0.07, 0.25)**	**0.001**	**0.006**	**0.32**	**0.07**	**0.16 (0.07, 0.25)**	**0.001**	**0.003**	**0.33**	**0.07**
Executive	**0.16 (0.02, 0.30)**	**0.024**	**0.029**	**0.21**	**0.04**	**0.16 (0.02, 0.30)**	**0.024**	**0.036**	**0.21**	**0.04**
Memory	**0.15 (0.06, 0.23)**	**0.001**	**0.003**	**0.29**	**0.07**	**0.15 (0.06, 0.23)**	**0.001**	**0.006**	**0.29**	**0.07**
Language	**0.17 (0.03, 0.30)**	**0.02**	**0.030**	**0.25**	**0.04**	**0.16 (0.03, 0.30)**	**0.021**	**0.025**	**0.25**	**0.04**
Attention	**0.16 (0.05, 0.27)**	**0.006**	**0.012**	**0.23**	**0.05**	**0.16 (0.05, 0.27)**	**0.006**	**0.012**	**0.24**	**0.05**
Visuomotor	0.13 (0.00, 0.27)	0.053	0.053	0.18	0.03	0.13 (0.00, 0.27)	0.056	0.056	0.19	0.03

Multivariable linear regression; Model A: adjusted for age, sex, years of education, estimated total intracranial volume and white matter hypointensities; Model B: Model A with additional adjustment for average whole-brain cortical thickness (n = 120–123). Beta estimates are represented per 1 standard deviation of FA in the hypothalamus, BH-p: Benjamini-Hochberg - adjusted p-value, R^2 - standard R^2 of the model, Delta R^2 - increase in model R^2 due to addition of hypothalamic FA. BH-adjusted p-values were calculated using the set of raw p-values represented in the Table, separately for Model A and B.

after the MRI. In total, there were 249 annual neurocognitive assessments, including 124 within 3 months of the MRI and 125 at least one year after the MRI (Table S1). In linear mixed effect models, hypothalamic FA was a significant independent positive predictor of the overall neurocognitive scores (beta [95 % CI] = 0.15 (0.07, 0.24), BH-adjusted p-value = 0.002), as well as memory, language, attention, and visuomotor cognitive domain scores (Table S14). Hypothalamic zMD was a significant negative predictor only for the language neurocognitive domain score but the p-value was not significant after the BH-adjustment (beta [95 % CI] = −0.17 (−0.31, −0.04), BH-adjusted p value = 0.08).

4. Discussion

Drawing on evidence from animal studies demonstrating the detrimental impact of hypothalamic aging on systemic aging, we set out to investigate the relationships of hypothalamic microstructure with brain structure and function in human aging. Using state-of-the-art MR diffusion imaging tailored to the anatomy of the aged brain, we found that 1) at older ages, the hypothalamus exhibits MRI characteristics that are consistent with altered microstructure, without observable age-related effects on hypothalamic volume; 2) MRI-derived hypothalamic microstructural features are associated with cortical thickness across multiple regions of the cortical mantle; 3) hypothalamic microstructural alterations and their relationship with cortical thickness are a feature of older age and are not observed in younger individuals; and 4) hypothalamic microstructural features are related to multi-domain neurocognitive performance, which was not explained by cortical thickness. The relationships between hypothalamic microstructure, cortical thickness and neurocognition were independent from microstructural features in other limbic regions that are functionally integrated with the hypothalamus and involved in neurocognition. This was the first study, to our knowledge, to demonstrate that aging-related MRI characteristics indexing hypothalamic microstructure may be a feature of neurocognitive aging in humans.

4.1. Hypothalamic microstructure varies with age and sex in older, but not younger adults

Development of MRI technology has allowed detection of microstructural changes in small brain volumes, such as the hypothalamus. We leveraged this technology to study subclinical, aging-related changes in the hypothalamus of older adults. MR diffusion imaging was utilized due to its high sensitivity in detecting microstructural changes, including neuroinflammation and gliosis (Budde et al., 2011; Hagen et al., 2007), which are the characteristics identified in the hypothalamus of aging animals (Zhang et al., 2013a). Two DTI parameters, MD and FA, were selected *a priori* for this analysis. Both capture multi-directional diffusion of water in the region of interest, but each provides qualitatively different information: MD measures overall magnitude of diffusion and FA measures directional coherence of anisotropic diffusion (Alexander et al., 2007). In our analyses, advanced age was associated with higher MD in the hypothalamus, which could be consistent with compromised microstructural integrity. Similar findings were noted in a study of over 550 adults (Thomas et al., 2019). Two other more recent cross-sectional studies (Spindler et al., 2023; Spindler and Thiel, 2022) did not find significant associations between age and MR diffusion metrics in the entire hypothalamic volume, although one of the studies reported a significant age-association in diffusion parameters in the anterior-superior hypothalamus (Spindler et al., 2023). The differences in the findings between studies may have resulted from variation in study populations. The studies that did not find significant age-associations in hypothalamic diffusion parameters included limited samples of adults at advanced ages (Spindler et al., 2023; Spindler and Thiel, 2022), which may have reduced the power to detect changes that occur in the later decades of life, when deterioration of brain structure and function accelerates. Indeed, in our study the association between age and hypothalamic MD was only observed in the older cohort (aged 65–97 years), while no significant association was found in the younger cohort (aged 18–63 years), suggesting that microstructural alterations in the hypothalamus represent a feature of later stages of neurocognitive aging. Intriguingly, while we did not find significant associations between age and hypothalamic FA, we found that women in the older cohort had significantly higher hypothalamic FA compared to men. Higher FA indicates greater directional coherence of water diffusion and is characteristic of healthy white matter. Our findings of higher FA in the hypothalamus of older women may suggests greater preservation of tissue organization in aging, consistent with findings in aged female mice (Debarba et al., 2022). It should be noted, however, that FA in gray matter structures, while studied in various conditions (Abe et al., 2008; Bouix et al., 2013; Stock et al., 2020) ought to be viewed as a sensitive marker of microstructural alteration, rather than an indicator of a specific pathologic process (or absence thereof).

4.2. Hypothalamic microstructural alteration is associated with cortical thickness in older, but not younger adults

In our analysis, greater hypothalamic MD was associated with lower cortical thickness in multiple brain regions. These associations were specific for the older cohort and were not observed in the younger and middle-aged participants. Reductions in cortical thickness are considered a sensitive measure for aging-related cortical atrophy, which involves the entire cortical mantle, with regional variations in severity, and accelerates after the age of 60 years (Storsve et al., 2014). The associations between hypothalamic MD and cortical thickness observed in our study largely followed cortical atrophy patterns associated with aging, with greatest effect sizes in medial orbitofrontal, frontal pole, inferior parietal, precuneus, inferior temporal, fusiform, and lateral occipital cortices (Lemaitre et al., 2012; Storsve et al., 2014). The associations between hypothalamic MD and cortical thickness were unchanged when MD from other limbic structures was added to our models; therefore, the observed associations related to hypothalamus

cannot be attributed to the decline in microstructural integrity of limbic system in general, supporting the hypothesis that aging of the hypothalamus may have a unique role in brain aging.

4.3. Hypothalamic microstructure is associated with cognition in older adults

Our analysis found strong associations between hypothalamic FA and overall, as well as domain-specific, neurocognitive performance, which was not explained by global cortical thickness. This finding is in contrast with a recent study that found no significant cross-sectional relationships between hypothalamic MR diffusion metrics and cognition (Spindler and Thiel, 2022). The differences in the findings may be explained by two major differences in study designs. First, the LonGenity Brain MRI cohort which participated in our study was composed exclusively of older adults in the later decades of life when neurocognitive aging is accelerated. The aforementioned study (Spindler and Thiel, 2022) included individuals from adolescence to older ages, which could reduce power to detect neurocognitive decline that results from aging. Second, our analysis utilized a robust neurocognitive assessment with standardized neuropsychological measures, designed to provide high sensitivity and specificity to detect aging-related neurocognitive dysfunction that may not meet criteria for cognitive impairment. On the other hand, the Addenbrooke's Cognitive Examination (ACE-R), utilized to assess cognition in the aforementioned study, is a brief screening test that was designed and validated as a clinical tool to detect mild dementia and differentiate between Alzheimer's disease and frontotemporal dementia (Mathuranath et al., 2000). Therefore, the study population and neurocognitive assessments employed in our analysis maximized the sensitivity to detect relationships between hypothalamic microstructure and cognition in the context of neurocognitive aging.

Notably, our analysis identified that hypothalamic MD and FA were associated with different neurocognitive aging parameters. MD and FA are mathematically related (Alexander et al., 2007) and increase in FA is often accompanied by decrease in MD (and vice versa), therefore it may be intuitively expected that they associate with the same parameters, albeit in opposite directions. However, even though FA and MD are mathematically related, this does not imply that their linear correlations with other parameters will be identical. In one study, white matter FA was overall negatively associated, and MD was positively associated with age, but with notable regional differences and time dissociations; for instance, while changes in the FA were observed in middle-aged, changes in MD were not apparent until older ages (Giorgio et al., 2010). It is thus not necessarily surprising that, in our analysis, we observed different linear associations of hypothalamic MD and FA with different features of neurocognitive aging.

4.4. Postulated mechanisms for relationships between the hypothalamus and neurocognitive aging

Given that our findings are mostly cross-sectional, we cannot draw conclusions about the mechanisms underlying the observed associations. A possibility of reverse causation or an existence of a common underlying mechanism for both hypothalamic microstructural alterations and features of neurocognitive aging cannot be excluded with certainty. It is plausible, however, that aging of the hypothalamus affects brain aging, which is supported by several lines of evidence from animal models and humans.

Aging of the hypothalamus may directly affect the rest of the brain. For instance, lateral hypothalamus modulates levels of arousal and motivation and is thought to be directly involved in certain types of learning and memory (Burdakov and Peleg-Raibstein, 2020); therefore, microstructural deterioration of the lateral hypothalamus could adversely affect neurocognitive performance in aging. Furthermore, in mice, aging-related microinflammation and gliosis in the hypothalamus deplete hypothalamic neurogenic stem/progenitor cell pools, which was postulated to adversely impact global neurogenesis in the brain (Zhang et al., 2017), although the presence of the neurogenic stem/progenitor cell in human hypothalamus remains to be determined. Aging of the hypothalamus may also affect the rest of the brain indirectly, through dysregulation of physiologic functions under hypothalamic control, including impairments in energy and glucose homeostasis, dysregulation of neuroendocrine pathways implicated in longevity (including GH/IGF-1, thyroid, gonadal and adrenal axes) (Brown-Borg, 2007; Zhang et al., 2013b), circadian dysfunction (Chang and Guarente, 2013) or altered sympathetic nervous system tone and hypertension (Purkayastha et al., 2011a). For instance, animal and human data implicate hypothalamic gliosis in obesity (Schur et al., 2015; Thaler et al., 2012) and glucose intolerance (Purkayastha et al., 2011b; Rosenbaum et al., 2022), which are associated with reductions in brain volumes and neurocognitive decline (Antal et al., 2022; Taki et al., 2011). In our analysis, associations between hypothalamic microstructure and either obesity, glycemia or history of diabetes/hypertension were not significant, which is not surprising given the overall preserved metabolic health of the study cohort. Alternatively, it is possible that factors other than metabolic dysfunction play a predominant role in brain aging among individuals who successfully reach more advanced age.

4.5. Limitations

Our study has unique strengths, but its several limitations should also be noted. First, the cross-sectional design does not allow establishing causality or temporal relationships of the observed associations. However, establishing rigorous cross-sectional associations in aging human cohorts is a necessary first step towards translating novel fundamental aging biology findings into humans, which can then help to identify actionable targets for slowing aging and its related morbidity. Our exploratory analysis which included longitudinal cognitive assessments supports the temporal relationship in which alteration of hypothalamic microstructure precedes cognitive decline. Second, the exact histologic correlates of the observed differences in hypothalamic MRI diffusion parameters are unknown. Studies in animal models point to the central role of hypothalamic gliosis in aging, while alterations of MRI diffusion metrics have been associated with histological evidence of gliosis in animals (Budde et al., 2011) and clinical evidence of gliosis in humans (Hagen et al., 2007). It is therefore plausible that microstructural changes detected with MRI diffusion metrics in our study correlate with gliosis in the hypothalamus. Future studies are needed to pursue more detailed analysis of the nature of the observed microstructural alterations in the hypothalamus. Third, given the proximity of the hypothalamus to the third ventricle, confounding of DTI metrics with CSF needs to be considered, due to possible inaccuracies in image registration, segmentation, or partial volume effects at the CSF border, which theoretically could be exacerbated in older individuals due to hypothalamic atrophy. For this reason, our automated segmentation procedure was specifically developed and validated in older adults. As a result, sensitivity of hypothalamic DTI metrics in our analysis was sufficient for detection of microstructural alterations relevant to features of neurocognitive aging. We did not find dependency of hypothalamic volume on age or on hypothalamic diffusion metrics, and when diffusion metrics were limited to the hypothalamic region distant from the CSF border, similar age-associations were observed. Furthermore, associations between hypothalamic diffusion metrics and features of neurocognitive aging were significant above and beyond any associations with age. We therefore conclude that observed relationships between hypothalamic diffusion metrics, age and neurocognitive aging cannot be explained by age-biased partial volume effects. To gain further insights into the pathophysiology underlying the observed diffusion changes in the hypothalamus, such as the presence of extracellular water, future studies may consider using acquisition protocols with optimized sensitivity to high diffusion (Hoy et al., 2014), which would allow for a comparison of diffusion tissue models without and with free water

elimination. A free water elimination procedure may also be considered, with an appropriate data acquisition, to enhance sensitivity of DTI metrics to detect subtle longitudinal changes in hypothalamic DTI parameters (Albi et al., 2017; Bergamino et al., 2016; Hoy et al., 2014). Fourth, we used theoretically derived cognitive composites, instead of an alternative approach of deriving cognitive composites with an empirical, data-driven approach. While empirical approach may more precisely map individual test scores to cognitive domains in a specific dataset, it does not clearly outperform theoretical approach and may be overly specific for a dataset and statistical method (Gibbons et al., 2012; Jonaitis et al., 2019; Wilhalme et al., 2017). Theory-based mapping of individual tests to cognitive domains is clinically relatable and may be more feasibly reproduced in other cohorts, although generalizability of specific domains needs to be carefully considered in the context of neurocognitive tasks that comprised each domain; for instance, attention and visuomotor domains in our analysis are overlapping and results could differ if one were to include different attention and visuomotor speed tasks. Fifth, we used FreeSurfer-generated white matter hypointensities on T1-weighted images, which may underestimate white matter lesion burden compared to T2-weighted-FLAIR-based white matter hyperintensity measurement, although prior studies have found that hypointensities may be a better (Haller et al., 2013) or equivalent (Wei et al., 2019) approach. However, sensitivity analysis using T2-weighted-FLAIR-based Age-Related White Matter Changes scale of hyperintensity volume, did not alter the pattern of results. Sixth, we analyzed a study cohort with overall preserved metabolic health, which limited the power to detect previously observed associations of hypothalamic diffusion parameters with obesity. However, to meet the study goal of establishing the relationships between hypothalamic and neurocognitive aging, it was advantageous to study a cohort with limited confounding by metabolically unhealthy aging. Finally, the LonGenity Brain MRI study cohort has a unique ethnic and socioeconomic composition, which can raise the question of generalizability of our results. Nevertheless, greater homogeneity of the study population may give us the power to detect biological associations. Furthermore, the findings from LonGenity have been previously validated in other cohorts (Rozing et al., 2010; Vergani et al., 2006); thus, the results from this study may likewise be generalizable.

5. Conclusions

To our knowledge, this is the first study to demonstrate that MRI characteristics of the hypothalamus consistent with aging-related microstructural alteration are associated with features of neurocognitive aging in humans. These findings provide evidence in support of further studies to elucidate the role of the hypothalamus in human aging, with a goal of developing interventions targeted at preserving hypothalamic structure and function to prolong health span in humans.

CRediT authorship contribution statement

Erica F. Weiss: Writing – review & editing, Methodology, Investigation, Conceptualization. **Timothy Darby:** Writing – review & editing, Investigation. **Noa Tal:** Writing – review & editing, Investigation. **Shira M. Siegel:** Data curation. **Roman Fleysher:** Writing – review & editing, Methodology, Formal analysis, Data curation, Conceptualization. **Kenny Q. Ye:** Writing – review & editing, Methodology. **Sandra Aleksic:** Writing – original draft, Visualization, Methodology, Investigation, Funding acquisition, Formal analysis, Conceptualization. **Juan Vazquez:** Writing – review & editing, Investigation. **Sofiya Milman:** Writing – review & editing, Resources, Methodology, Funding acquisition, Conceptualization. **Michael L Lipton:** Writing – review & editing, Methodology, Funding acquisition, Conceptualization. **Nir Barzilai:** Writing – review & editing, Resources, Methodology, Conceptualization. **Tina Gao:** Writing – review & editing, Project administration, Data curation. **Helena M. Blumen:** Writing – review & editing, Methodology, Conceptualization.

Declaration of Competing Interest

None.

Acknowledgements

We thank all the participants and research teams of the LonGenity and Lifespan studies. This work was supported by the National Institute on Aging at the National Institutes of Health (grant numbers 1K76AG083274 to S.A., R01AG061155 and R56AG044829 to S.M., R01AG062659 to H.M.B., P01AG021654 and R01AG057909 to N.B.), the National Center for Advancing Translational Sciences at the National Institutes of Health (KL2TR002558 to S.A.), National Institute on Neurological Disorders and Stroke at the National Institues of Health (R01NS123445 and R01NS123374 to M.L.L.) and the Einstein-Paul Glenn Foundation for Medical Research Center for the Biology of Human Aging to N. B. The funding resources did not have any involvement in the study design, collection, analysis and interpretation of data, writing of the report, or the decision to submit the article for publication.

Verification

We hereby verify that the work described in this manuscript has not been published previously, that it is not under consideration for publication elsewhere, that its publication is approved by all authors and explicitly by the responsible authorities where the work was carried out (Albert Einstein College of Medicine Institutional Review Board), and that, if accepted, it will not be published elsewhere in the same form, in English or in any other language, including electronically without the written consent of the copyright-holder.

Appendix A. Supporting information

Supplementary data associated with this article can be found in the online version at doi:10.1016/j.neurobiolaging.2024.05.018.

References

Abe, O., Yamasue, H., Aoki, S., Suga, M., Yamada, H., Kasai, K., Masutani, Y., Kato, N., Ohtomo, K., 2008. Aging in the CNS: comparison of gray/white matter volume and diffusion tensor data. Neurobiol. Aging 29 (1), 102–116.

Albi, A., Pasternak, O., Minati, L., Marizzoni, M., Bartrés-Faz, D., Bargalló, N., Bosch, B., Rossini, P.M., Marra, C., Müller, B., Fiedler, U., Wiltfang, J., Roccatagliata, L., Picco, A., Nobili, F.M., Blin, O., Sein, J., Ranjeva, J.P., Didic, M., Bombois, S., Lopes, R., Bordet, R., Gros-Dagnac, H., Payoux, P., Zoccatelli, G., Alessandrini, F., Beltramello, A., Ferretti, A., Caulo, M., Aiello, M., Cavaliere, C., Soricelli, A., Parnetti, L., Tarducci, R., Floridi, P., Tsolaki, M., Constantinidis, M., Drevelegas, A., Frisoni, G., Jovicich, J., Consortium, P., 2017. Free water elimination improves test-retest reproducibility of diffusion tensor imaging indices in the brain: A longitudinal multisite study of healthy elderly subjects. Hum. Brain Mapp. 38 (1), 12–26.

Alexander, A.L., Lee, J.E., Lazar, M., Field, A.S., 2007. Diffusion tensor imaging of the brain. Neurotherapeutics 4 (3), 316–329.

Antal, B., McMahon, L.P., Sultan, S.F., Lithen, A., Wexler, D.J., Dickerson, B., Ratai, E.M., Mujica-Parodi, L.R., 2022. Type 2 diabetes mellitus accelerates brain aging and cognitive decline: Complementary findings from UK Biobank and meta-analyses. Elife 11.

Avants, B.B., Tustison, N.J., Song, G., Cook, P.A., Klein, A., Gee, J.C., 2011. A reproducible evaluation of ANTs similarity metric performance in brain image registration. Neuroimage 54 (3), 2033–2044.

Avants, B.B., Tustison, N.J., Stauffer, M., Song, G., Wu, B., Gee, J.C., 2014. The Insight ToolKit image registration framework. Front Neuroinform 8, 44.

Bergamino, M., Pasternak, O., Farmer, M., Shenton, M.E., Hamilton, J.P., 2016. Applying a free-water correction to diffusion imaging data uncovers stress-related neural pathology in depression. Neuroimage Clin. 10, 336–342.

Bouix, S., Pasternak, O., Rathi, Y., Pelavin, P.E., Zafonte, R., Shenton, M.E., 2013. Increased gray matter diffusion anisotropy in patients with persistent post-concussive symptoms following mild traumatic brain injury. PLoS One 8 (6), e66205.

Brown-Borg, H.M., 2007. Hormonal regulation of longevity in mammals. Ageing Res Rev. 6 (1), 28–45.

Budde, M.D., Janes, L., Gold, E., Turtzo, L.C., Frank, J.A., 2011. The contribution of gliosis to diffusion tensor anisotropy and tractography following traumatic brain injury: validation in the rat using Fourier analysis of stained tissue sections. Brain 134 (Pt 8), 2248–2260.
Burdakov, D., Peleg-Raibstein, D., 2020. The hypothalamus as a primary coordinator of memory updating. Physiol. Behav. 223, 112988.
Buschke, H., Kuslansky, G., Katz, M., Stewart, W.F., Sliwinski, M.J., Eckholdt, H.M., Lipton, R.B., 1999. Screening for dementia with the memory impairment screen. Neurology 52 (2), 231–238.
Buschke, H., Sliwinski, M.J., Kuslansky, G., Katz, M., Verghese, J., Lipton, R.B., 2006. Retention weighted recall improves discrimination of Alzheimer's disease. J. Int. Neuropsychol. Soc.: JINS 12 (3), 436–440.
Chang, H.C., Guarente, L., 2013. SIRT1 mediates central circadian control in the SCN by a mechanism that decays with aging. Cell 153 (7), 1448–1460.
Chen, K.X., Worley, S., Foster, H., Edasery, D., Roknsharifi, S., Ifrah, C., Lipton, M.L., 2021. Oral contraceptive use is associated with smaller hypothalamic and pituitary gland volumes in healthy women: A structural MRI study. PLoS One 16 (4), e0249482.
Cox, R.W., 1996. AFNI: software for analysis and visualization of functional magnetic resonance neuroimages. Comput. Biomed. Res 29 (3), 162–173.
Dale, A.M., Fischl, B., Sereno, M.I., 1999. Cortical surface-based analysis. I. Segmentation and surface reconstruction. Neuroimage 9 (2), 179–194.
Debarba, L.K., Jayarathne, H.S.M., Miller, R.A., Garratt, M., Sadagurski, M., 2022. 17-α-Estradiol Has Sex-Specific Effects on Neuroinflammation That Are Partly Reversed by Gonadectomy. J. Gerontol. A Biol. Sci. Med Sci. 77 (1), 66–74.
den Heijer, T., der Lijn, F., Vernooij, M.W., de Groot, M., Koudstaal, P.J., van der Lugt, A., Krestin, G.P., Hofman, A., Niessen, W.J., Breteler, M.M., 2012. Structural and diffusion MRI measures of the hippocampus and memory performance. Neuroimage 63 (4), 1782–1789.
Desikan, R.S., Segonne, F., Fischl, B., Quinn, B.T., Dickerson, B.C., Blacker, D., Buckner, R.L., Dale, A.M., Maguire, R.P., Hyman, B.T., Albert, M.S., Killiany, R.J., 2006. An automated labeling system for subdividing the human cerebral cortex on MRI scans into gyral based regions of interest. Neuroimage 31 (3), 968–980.
Fleysher, R., Lipton, M.L., Noskin, O., Rundek, T., Lipton, R., Derby, C.A., 2018. White matter structural integrity and transcranial Doppler blood flow pulsatility in normal aging. Magn. Reson Imaging 47, 97–102.
Gibbons, L.E., Carle, A.C., Mackin, R.S., Harvey, D., Mukherjee, S., Insel, P., Curtis, S.M., Mungas, D., Crane, P.K., Initiative, As.D.N., 2012. A composite score for executive functioning, validated in Alzheimer's Disease Neuroimaging Initiative (ADNI) participants with baseline mild cognitive impairment. Brain Imaging Behav. 6 (4), 517–527.
Giorgio, A., Santelli, L., Tomassini, V., Bosnell, R., Smith, S., De Stefano, N., Johansen-Berg, H., 2010. Age-related changes in grey and white matter structure throughout adulthood. Neuroimage 51 (3), 943–951.
Glasser, M.F., Sotiropoulos, S.N., Wilson, J.A., Coalson, T.S., Fischl, B., Andersson, J.L., Xu, J., Jbabdi, S., Webster, M., Polimeni, J.R., Van Essen, D.C., Jenkinson, M., Consortium, W.U.-M.H., 2013. The minimal preprocessing pipelines for the Human Connectome Project. Neuroimage 80, 105–124.
Greve, D.N., Fischl, B., 2009. Accurate and robust brain image alignment using boundary-based registration. Neuroimage 48 (1), 63–72.
Gubbi, S., Schwartz, E., Crandall, J., Verghese, J., Holtzer, R., Atzmon, G., Braunstein, R., Barzilai, N., Milman, S., 2017. Effect of Exceptional Parental Longevity and Lifestyle Factors on Prevalence of Cardiovascular Disease in Offspring. Am. J. Cardiol. 120 (12), 2170–2175.
Habes, M., Erus, G., Toledo, J.B., Zhang, T., Bryan, N., Launer, L.J., Rosseel, Y., Janowitz, D., Doshi, J., Van der Auwera, S., von Sarnowski, B., Hegenscheid, K., Hosten, N., Homuth, G., Volzke, H., Schminke, U., Hoffmann, W., Grabe, H.J., Davatzikos, C., 2016. White matter hyperintensities and imaging patterns of brain ageing in the general population. Brain 139 (Pt 4), 1164–1179.
Hagen, T., Ahlhelm, F., Reiche, W., 2007. Apparent diffusion coefficient in vasogenic edema and reactive astrogliosis. Neuroradiology 49 (11), 921–926.
Haller, S., Kövari, E., Herrmann, F.R., Cuvinciuc, V., Tomm, A.M., Zulian, G.B., Lovblad, K.O., Giannakopoulos, P., Bouras, C., 2013. Do brain T2/FLAIR white matter hyperintensities correspond to myelin loss in normal aging? A radiologic-neuropathologic correlation study. Acta Neuropathol. Commun. 1, 14.
Goodglass, H., Kaplan, E., 1983. The assessment of aphasia and related disorders, 2nd ed ed. Lea & Febiger, Philadelphia.
Hoy, A.R., Koay, C.G., Kecskemeti, S.R., Alexander, A.L., 2014. Optimization of a free water elimination two-compartment model for diffusion tensor imaging. Neuroimage 103, 323–333.
Jenkinson, M., Beckmann, C.F., Behrens, T.E., Woolrich, M.W., Smith, S.M., 2012. FSL. Neuroimage 62 (2), 782–790.
Jiang, Y., Tian, Y., Wang, Z., 2019. Age-Related Structural Alterations in Human Amygdala Networks: Reflections on Correlations Between White Matter Structure and Effective Connectivity. Front Hum. Neurosci. 13, 214.
Jonaitis, E.M., Koscik, R.L., Clark, L.R., Ma, Y., Betthauser, T.J., Berman, S.E., Allison, S. L., Mueller, K.D., Hermann, B.P., Van Hulle, C.A., Christian, B.T., Bendlin, B.B., Blennow, K., Zetterberg, H., Carlsson, C.M., Asthana, S., Johnson, S.C., 2019. Measuring longitudinal cognition: Individual tests versus composites. Alzheimers Dement (Amst. 11, 74–84.
Klein, A., Tourville, J., 2012. 101 labeled brain images and a consistent human cortical labeling protocol. Front Neurosci. 6, 171.
Lemaitre, H., Goldman, A.L., Sambataro, F., Verchinski, B.A., Meyer-Lindenberg, A., Weinberger, D.R., Mattay, V.S., 2012. Normal age-related brain morphometric changes: nonuniformity across cortical thickness, surface area and gray matter volume? Neurobiol. Aging 33 (3), 617.e611-619.
Leng, L., Yuan, Z., Su, X., Chen, Z., Yang, S., Chen, M., Zhuang, K., Lin, H., Sun, H., Li, H., Xue, M., Xu, J., Yan, J., Yuan, T., Zhang, J., 2023. Hypothalamic Menin regulates systemic aging and cognitive decline. PLoS Biol. 21 (3), e3002033.
Mathuranath, P.S., Nestor, P.J., Berrios, G.E., Rakowicz, W., Hodges, J.R., 2000. A brief cognitive test battery to differentiate Alzheimer's disease and frontotemporal dementia. Neurology 55 (11), 1613–1620.
Melmed, S., 2016. Williams Textbook of Endocrinology, 13th ed. Elsevier.
Puig, J., Blasco, G., Daunis, I.E.J., Molina, X., Xifra, G., Ricart, W., Pedraza, S., Fernandez-Aranda, F., Fernandez-Real, J.M., 2015. Hypothalamic damage is associated with inflammatory markers and worse cognitive performance in obese subjects. J. Clin. Endocrinol. Metab. 100 (2), E276–E281.
Purkayastha, S., Zhang, G., Cai, D., 2011a. Uncoupling the mechanisms of obesity and hypertension by targeting hypothalamic IKK-beta and NF-kappaB. Nat. Med 17 (7), 883–887.
Purkayastha, S., Zhang, H., Zhang, G., Ahmed, Z., Wang, Y., Cai, D., 2011b. Neural dysregulation of peripheral insulin action and blood pressure by brain endoplasmic reticulum stress. Proc. Natl. Acad. Sci. USA 108 (7), 2939–2944.
Reitan, R.M., 1955. The relation of the trail making test to organic brain damage. J. Consult. Psychol. 19 (5), 393–394.
Rosenbaum, J.L., Melhorn, S.J., Schoen, S., Webb, M.F., De Leon, M.R.B., Humphreys, M., Utzschneider, K.M., Schur, E.A., 2022. Evidence That Hypothalamic Gliosis Is Related to Impaired Glucose Homeostasis in Adults With Obesity. Diabetes Care 45 (2), 416–424.
Rozing, M.P., Houwing-Duistermaat, J.J., Slagboom, P.E., Beekman, M., Frolich, M., de Craen, A.J., Westendorp, R.G., van Heemst, D., 2010. Familial longevity is associated with decreased thyroid function. J. Clin. Endocrinol. Metab. 95 (11), 4979–4984.
Sadagurski, M., Cady, G., Miller, R.A., 2017. Anti-aging drugs reduce hypothalamic inflammation in a sex-specific manner. Aging Cell 16 (4), 652–660.
Sadagurski, M., Landeryou, T., Cady, G., Bartke, A., Bernal-Mizrachi, E., Miller, R.A., 2015a. Transient early food restriction leads to hypothalamic changes in the long-lived crowded litter female mice. Physiol. Rep. 3 (4).
Sadagurski, M., Landeryou, T., Cady, G., Kopchick, J.J., List, E.O., Berryman, D.E., Bartke, A., Miller, R.A., 2015b. Growth hormone modulates hypothalamic inflammation in long-lived pituitary dwarf mice. Aging Cell 14 (6), 1045–1054.
Schur, E.A., Melhorn, S.J., Oh, S.K., Lacy, J.M., Berkseth, K.E., Guyenet, S.J., Sonnen, J. A., Tyagi, V., Rosalynn, M., De Leon, B., Webb, M.F., Gonsalves, Z.T., Fligner, C.L., Schwartz, M.W., Maravilla, K.R., 2015. Radiologic evidence that hypothalamic gliosis is associated with obesity and insulin resistance in humans. Obes. (Silver Spring) 23 (11), 2142–2148.
Smith, S.M., Jenkinson, M., Woolrich, M.W., Beckmann, C.F., Behrens, T.E., Johansen-Berg, H., Bannister, P.R., De Luca, M., Drobnjak, I., Flitney, D.E., Niazy, R.K., Saunders, J., Vickers, J., Zhang, Y., De Stefano, N., Brady, J.M., Matthews, P.M., 2004. Advances in functional and structural MR image analysis and implementation as FSL. Neuroimage 23 (Suppl 1), S208–S219.
Spindler, M., Palombo, M., Zhang, H., Thiel, C.M., 2023. Dysfunction of the hypothalamic-pituitary adrenal axis and its influence on aging: the role of the hypothalamus. Sci. Rep. 13 (1), 6866.
Spindler, M., Thiel, C.M., 2022. Hypothalamic microstructure and function are related to body mass, but not mental or cognitive abilities across the adult lifespan. Geroscience.
Stern, Y., Andrews, H., Pittman, J., Sano, M., Tatemichi, T., Lantigua, R., Mayeux, R., 1992. Diagnosis of dementia in a heterogeneous population. Development of a neuropsychological paradigm-based diagnosis of dementia and quantified correction for the effects of education. Arch. Neurol. 49 (5), 453–460.
Stock, B., Shrestha, M., Seiler, A., Foerch, C., Hattingen, E., Steinmetz, H., Deichmann, R., Wagner, M., Gracien, R.M., 2020. Distribution of Cortical Diffusion Tensor Imaging Changes in Multiple Sclerosis. Front Physiol. 11, 116.
Storsve, A.B., Fjell, A.M., Tamnes, C.K., Westlye, L.T., Overbye, K., Aasland, H.W., Walhovd, K.B., 2014. Differential longitudinal changes in cortical thickness, surface area and volume across the adult life span: regions of accelerating and decelerating change. J. Neurosci. 34 (25), 8488–8498.
Taki, Y., Kinomura, S., Sato, K., Goto, R., Kawashima, R., Fukuda, H., 2011. A longitudinal study of gray matter volume decline with age and modifying factors. Neurobiol. Aging 32 (5), 907–915.
Thaler, J.P., Yi, C.X., Schur, E.A., Guyenet, S.J., Hwang, B.H., Dietrich, M.O., Zhao, X., Sarruf, D.A., Izgur, V., Maravilla, K.R., Nguyen, H.T., Fischer, J.D., Matsen, M.E., Wisse, B.E., Morton, G.J., Horvath, T.L., Baskin, D.G., Tschop, M.H., Schwartz, M.W., 2012. Obesity is associated with hypothalamic injury in rodents and humans. J. Clin. Invest 122 (1), 153–162.
Thomas, K., Beyer, F., Lewe, G., Zhang, R., Schindler, S., Schonknecht, P., Stumvoll, M., Villringer, A., Witte, A.V., 2019. Higher body mass index is linked to altered hypothalamic microstructure. Sci. Rep. 9 (1), 17373.
Tustison, N.J., Cook, P.A., Klein, A., Song, G., Das, S.R., Duda, J.T., Kandel, B.M., van Strien, N., Stone, J.R., Gee, J.C., Avants, B.B., 2014. Large-scale evaluation of ANTs and FreeSurfer cortical thickness measurements. Neuroimage 99, 166–179.
Vergani, C., Lucchi, T., Caloni, M., Ceconi, I., Calabresi, C., Scurati, S., Arosio, B., 2006. I405V polymorphism of the cholesteryl ester transfer protein (CETP) gene in young and very old people. Arch. Gerontol. Geriatr. 43 (2), 213–221.
Wahlund, L.O., Barkhof, F., Fazekas, F., Bronge, L., Augustin, M., Sjögren, M., Wallin, A., Ader, H., Leys, D., Pantoni, L., Pasquier, F., Erkinjuntti, T., Scheltens, P., European Task Force on Age-Related White Matter Changes, 2001. A new rating scale for age-related white matter changes applicable to MRI and CT. Stroke 32 (6), 1318–1322.
Wechsler, D., 1981 Wechsler adult intelligence scale - revised (WAIS-R). Psychological Corporation, New York.
Wechsler, D., 1987. Manual for the Wechsler Memory Scale-Revised (WMS-R). The Psychological Corporation, San Antonio, TX.

Wei, K., Tran, T., Chu, K., Borzage, M.T., Braskie, M.N., Harrington, M.G., King, K.S., 2019. White matter hypointensities and hyperintensities have equivalent correlations with age and CSF β-amyloid in the nondemented elderly. Brain Behav. 9 (12), e01457.

Wen, W., Sachdev, P.S., Chen, X., Anstey, K., 2006. Gray matter reduction is correlated with white matter hyperintensity volume: a voxel-based morphometric study in a large epidemiological sample. Neuroimage 29 (4), 1031–1039.

Wilhalme, H., Goukasian, N., De Leon, F., He, A., Hwang, K.S., Woo, E., Elashoff, D., Zhou, Y., Ringman, J.M., Apostolova, L.G., 2017. A comparison of theoretical and statistically derived indices for predicting cognitive decline. Alzheimers Dement (Amst. 6, 171–181.

Woolrich, M.W., Jbabdi, S., Patenaude, B., Chappell, M., Makni, S., Behrens, T., Beckmann, C., Jenkinson, M., Smith, S.M., 2009. Bayesian analysis of neuroimaging data in FSL. Neuroimage 45 (1 Suppl), S173–S186.

Yang, S.B., Tien, A.C., Boddupalli, G., Xu, A.W., Jan, Y.N., Jan, L.Y., 2012. Rapamycin ameliorates age-dependent obesity associated with increased mTOR signaling in hypothalamic POMC neurons. Neuron 75 (3), 425–436.

Yekutieli, D., Benjamini, Y., 1999. Resampling-based false discovery rate controlling multiple test procedures for correlated test statistics. J. Stat. Plan. Inference 82, 171–196.

Zhang, G., Li, J., Purkayastha, S., Tang, Y., Zhang, H., Yin, Y., Li, B., Liu, G., Cai, D., 2013a. Hypothalamic programming of systemic ageing involving IKK-beta, NF-kappaB and GnRH. Nature 497 (7448)), 211–216.

Zhang, G., Li, J., Purkayastha, S., Tang, Y., Zhang, H., Yin, Y., Li, B., Liu, G., Cai, D., 2013b. Hypothalamic programming of systemic ageing involving IKK-β, NF-κB and GnRH. Nature 497 (7448)), 211–216.

Zhang, Y., Kim, M.S., Jia, B., Yan, J., Zuniga-Hertz, J.P., Han, C., Cai, D., 2017. Hypothalamic stem cells control ageing speed partly through exosomal miRNAs. Nature 548 (7665)), 52–57.